Vibronic and magnetic excitations in the spin-orbital liquid state of FeSc2S4

Alexander Krimmel, M. Mücksch, Vladimir Tsurkan, M. M. Koza, H. Mutka, Alois Loidl

Angaben zur Veröffentlichung / Publication details:

Krimmel, Alexander, M. Mücksch, Vladimir Tsurkan, M. M. Koza, H. Mutka, and Alois Loidl. 2005. "Vibronic and magnetic excitations in the spin-orbital liquid state of FeSc2S4." *Physical Review Letters* 94 (23): 237402. https://doi.org/10.1103/PhysRevLett.94.237402.

Vibronic and Magnetic Excitations in the Spin-Orbital Liquid State of $FeSc_2S_4$

A. Krimmel,[1] M. Mücksch,[2,3] V. Tsurkan,[1,4] M. M. Koza,[3] H. Mutka,[3] and A. Loidl[1]

[1]*Experimentalphysik V, Center for Electronic Correlations and Magnetism, Universität Augsburg, D - 86159 Augsburg, Germany*
[2]*Experimentalphysik II, Institut für Physik, Universität Augsburg, D - 86159 Augsburg, Germany*
[3]*Institut Laue Langevin, BP 156 X, F - 38042 Grenoble Cedex 9, France*
[4]*Institute of Applied Physics, Academy of Science of Moldova, MD2028, Chisinau, Moldova*

(Received 15 June 2004; published 16 June 2005)

Inelastic neutron scattering results on the spin-orbital liquid in $FeSc_2S_4$ are presented. This sulfospinel reveals strong geometric frustration in the spin and in the orbital sector. In the present experiments the orbital liquid is evidenced by a clear spectroscopic signature of a dynamic Jahn-Teller effect with a vibronic splitting $3\Gamma \approx 2$ meV in agreement with theoretical estimates. The excitations of the spin liquid reveal strong dispersion and can be characterized as cooperative spin excitations in a supercooled paramagnet with a spin gap of $\Delta \approx 0.2$ meV.

DOI: 10.1103/PhysRevLett.94.237402 PACS numbers: 78.70.Nx, 71.70.−d, 75.40.Gb, 75.50.Mm

Exchange interactions between the internal degrees of freedom, like spin or orbital moments, generally result in long-range order. In insulating 3D systems long-range spin order is induced via superexchange interactions and long-range orbital order via the time-honored Jahn-Teller (JT) effect [1]. In orbitally degenerate systems orbital order can also be induced via a purely electronic mechanism, the so-called Kugel-Khomskii exchange [2]. Frustrated magnets, however, do not show long-range order despite strong interactions evidenced by high Curie-Weiss temperatures of the paramagnetic susceptibility. Frustration characterizes the inability of a system to establish an ordered ground state which results from the fact that neighboring moments cannot satisfy all pairwise interactions. For spin systems, frustration combined with bond or site disorder drives a spin-glass state [3]. But macroscopically degenerate ground states can also result from geometric frustration in pure stoichiometric compounds [4]. In this case the resulting ground state can be rather complex, and spin liquids (SL) [5], heavy-fermion behavior [6], clusters of spins [7], or spin-ice states [8,9] have been observed. While geometric frustration has been investigated in detail for spin systems (see, e.g., [4]), frustration in the orbital sector is not well established, and only recently the observation of an orbital liquid and an orbital glass has been reported for the ferrimagnet $FeCr_2S_4$ [10]. The ground state properties of a system can best be characterized by its excitations, and the experimental observation of the dynamics of a spin-orbital liquid (SOL) remains a challenge to solid-state physicists.

From susceptibility and heat capacity experiments a SL state has been deduced for $MnSc_2S_4$ and a SOL for $FeSc_2S_4$ [11]. In the latter compound Fe^{2+} is tetrahedrally coordinated by the sulfur ions and the $3d$ multiplett is split into a low-lying doublet (e) and an excited triplet (t_2). High-spin Fe^{2+} ($S = 2$) exhibits a hole in the lower doublet and is JT active. Hence one expects an antiferromagnetic (AFM) ground state, and in addition, a JT-derived structural phase transition which establishes orbital order at low temperatures. However, it has been shown that $FeSc_2S_4$ remains cubic and paramagnetic down to the lowest temperatures ($T > 50$ mK). Hence geometric frustration dominates both the spin and the orbital sector establishing a SOL ground state [11]. The magnetic frustration parameter defined as the ratio of the Curie-Weiss temperature $\theta_{CW} = -45$ K, corresponding to the strength of the leading exchange interactions to the upper limit of the magnetic ordering temperature, is of the order of 1000, one of the largest values ever observed.

There exists a number of neutron scattering experiments on geometrically frustrated spin systems: spin fluctuations with a characteristic energy width and a weak temperature dependence have been observed in metallic and frustrated $Y{:}ScMn_2$ and in geometrically frustrated β-Mn [12,13]. Competing ferromagnetic and AFM spin fluctuations occur in the quasielastic excitation spectrum of the frustrated heavy-fermion system LiV_2O_4 [6,14,15]. Turning to insulating frustrated magnets, for $ZnCr_2O_4$, with the Cr spins

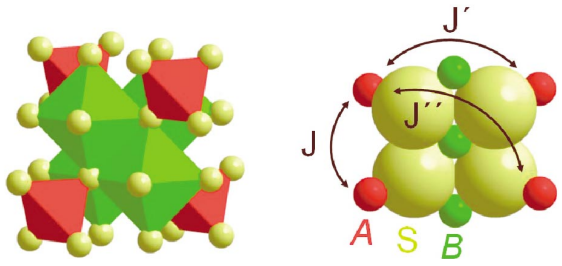

FIG. 1 (color). Coordination polyhedra of the spinel structure of $FeSc_2S_4$. A-site Fe (red) is embedded in a tetrahedral environment of sulfur (yellow), while B-site Sc has octahedral environment (left part). The A-site exchange is mediated via three different Fe-S-Sc-S-Fe interaction paths. A plaquette containing nearest, next nearest, and next-next nearest neighbors of the A-site sublattice with corresponding exchange constants J, J', and J'' is shown at the right.

residing on a pyrochlore lattice, Lee *et al.* [7] demonstrated that groups of six spins form weakly interacting AFM loops. In this communication we report inelastic neutron scattering experiments on polycrystalline $FeSc_2S_4$. We provide experimental evidence of spin and orbital derived excitations in the SOL state: the spin excitations are a paramount example of a liquidlike dynamic structure factor in a cooperative paramagnet. The orbital excitations can satisfactorily be explained by a dynamic Jahn-Teller effect.

Investigations of normal AB_2X_4 spinels with only A-A magnetic interactions are rare and only a few examples of long-range magnetic and orbital order are known. Roth [16] discussed the principal superexchange paths linking the A sites in the normal spinel. A schematic view of the spinel structure and the A-site magnetic exchange is shown in Fig. 1. The A-site ions in the normal spinel structure form a diamond lattice, consisting of two interpenetrating fcc sublattices which are highly frustrated. Looking for the exchange paths in detail, all superexchange paths involve at least three intermediate ions and therefore are certainly weak. Exchange J of the nearest neighbor (NN) and J' of the next nearest neighbor (NNN) A-site ions involve intermediate X-B-X ions with a bond angle close to 90°, whereas the next-next nearest neighbor (NNNN) exchange J'' contains X-B-X ions with a bond angle close to 180°. There are four NN with a sixfold interaction path and 12 NNN with a twofold interaction path, resulting in a multiplicity for J and J' of 24 each. The exchange paths J'' to the 12 NNNN are single fold. It should be stressed that although NN, NNN, and NNNN shells exhibit different spacings in the crystal lattice, the lengths of the exchange paths are rather similar. Therefore, the weak indirect interaction is strengthened by the large multiplicity of the exchange paths explaining the relatively high Curie-Weiss temperature of $FeSc_2S_4$.

Figure 2 shows an energy versus wave vector plot of the dynamic structure factor $S(Q, \omega)$ (all data have been normalized to vanadium standard and corrected for the neutron magnetic form factor) as observed by the thermal time-of-flight neutron spectrometer IN4 of polycrystalline $FeSc_2S_4$ at 1.6 K. Details of the sample preparation and characterization are given in Ref. [11]. The dynamic structure factor is proportional to the imaginary part of the generalized dynamic susceptibility via $S(Q, \omega) = [1 - \exp(-\hbar\omega/k_BT)]^{-1}\chi''(Q, \omega)$. A resolution limited narrow riff around zero energy transfer is observed due to elastic incoherent scattering. The dark points within this band correspond to highly enhanced intensities of nuclear Bragg reflections. The spinel-type structure of $FeSc_2S_4$ with lattice parameter $a = 10.52$ Å gives rise to nuclear Bragg scattering with the first reflections at $Q = 1.03$ Å^{-1} (111), 1.69 Å^{-1} (220), 1.98 Å^{-1} (311), 2.07 Å^{-1} (222), and 2.39 Å^{-1} (400). Beyond this band of elastic scattering, additional inelastic intensities are observed which are of magnetic origin, as inferred from the corresponding temperature and Q dependence, respectively. The magnetic intensities extend up to energies of approximately 5 meV (color scale of Fig. 2 above a background level encoded in blue) corresponding to the order of the magnetic exchange in the system. Two specific characteristics of $S(Q, \omega)$ can be observed: a modulation of the inelastic intensities as function of Q with somewhat enhanced intensities just between the Q values of the nuclear Bragg intensities indicating AFM fluctuations, and a rather abrupt change of intensity (color) around 2.5 meV signaling significant deviations from purely quasielastic magnetic intensities.

This is documented in Fig. 3 where a cut at $Q = 1.1$ Å^{-1} for 1.6 and 80 K is plotted and a clear inelastic contribution with excitation energies of approximately 2 meV is present. With decreasing temperature the excitation energies $\hbar\omega$ soften and the damping γ decreases

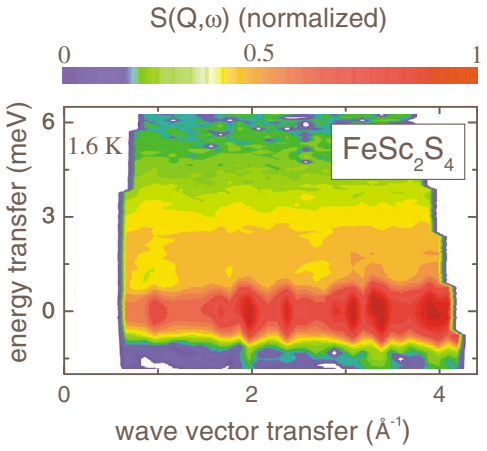

FIG. 2 (color). Contour plot $S(Q, \omega)$ of $FeSc_2S_4$ obtained by inelastic neutron scattering with an incident neutron energy of 17 meV at $T = 1.6$ K.

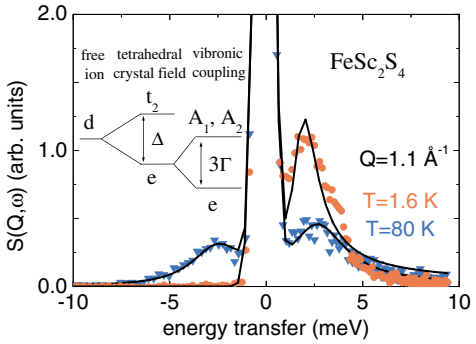

FIG. 3 (color). $S(Q, \omega)$ of $FeSc_2S_4$ at constant $Q = 1.1$ Å^{-1} at $T = 80$ K (blue triangles) and at $T = 1.6$ K (red circles) as derived from Fig. 2. The full black line is a fit to the data employing an elastic Gaussian and a single inelastic Lorentzian line, multiplied by the detailed balance factor and convoluted with the instrumental resolution. Inset: the dynamic Jahn-Teller effect is illustrated by the vibronic splitting 3Γ of electronic configuration in addition to the conventional crystal-field splitting.

($T = 80$ K: $\hbar\omega = 2.4$ meV, $\gamma = 1.6$ meV; $T = 1.5$ K: $\hbar\omega = 1.73$ meV, $\gamma = 0.80$ meV). This excitation is predominantly of magnetic origin as determined from the Q-dependent intensities, and in first approximation its spectral shape is independent of Q; e.g., width and shape are similar when measured at wave vectors close to or between nuclear Bragg reflections. We also performed a detailed neutron scattering study [17] on $MnSc_2S_4$ which orders magnetically close to 2 K and, needless to say, we did not observe a similar excitation. $MnSc_2S_4$ is a spin-only system and hence we interpret the observed excitation in $FeSc_2S_4$ as a signature of the orbital liquid state.

As outlined above, the electronic ground state of tetrahedrally coordinated Fe^{+2} is JT active. The static JT effect results from a strong coupling between the electronic and the lattice degrees of freedom, giving rise to orbital order and a long-range lattice distortion. If the coupling is weak no static distortion appears, but results in a coupled motion of electronic and vibrational modes, referred to as dynamic JT effect and described for the single ion case by Ham [18]. In this most simple situation, which is depicted in the inset of Fig. 3, the electronic ground state remains an e state, separated by 3Γ from the first excited vibronic levels A_1 and A_2. The single ion situation was further treated in detail by Slack *et al.* [19], Feiner [20], and Testelin *et al.* [21] including the effect of spin-orbit coupling. In this case the transition to the lowest excited state of the vibronic level scheme is magnetic dipole active and therefore observable by neutron scattering. Its energy as observed for Fe^{+2} in CdTe (1.6 meV [21]) is rather close to the value found for $FeSc_2S_4$. For the title compound, Brossard *et al.* [22] have demonstrated that only the inclusion of spin-orbit coupling as well as random strains can explain the quadrupole splitting observed in Mössbauer experiments [22]. The semiquantitative agreement with the single ion calculations within the framework of a dynamic Jahn-Teller effect, as well as the experimental observations on diluted systems and in $FeSc_2S_4$, provide strong support to our interpretation of the excitations in $FeSc_2S_4$ in terms of an excitation to the lowest magnetic state of the vibronic level scheme. Of course, we cannot expect that the single ion level scheme is the complete explanation for the exchange coupled system investigated in the present work. Especially the notable broadening of the magnetic response points out to the presence of magnetic exchange. The consequences of this collective situation will be detailed below.

Turning to a discussion of the low-energy AFM spin fluctuations, Fig. 4 presents a contour plot of $S(Q, \omega)$ at 80 K (upper panel) and at 1.6 K (lower panel) as obtained on the high-resolution time-of-flight spectrometer IN6, zooming into the low-Q and low-energy-transfer region not resolved in Fig. 2. Now the strong modulation with Q and the associated softening at specific Q points becomes evident. The first three nuclear Bragg reflections are visible

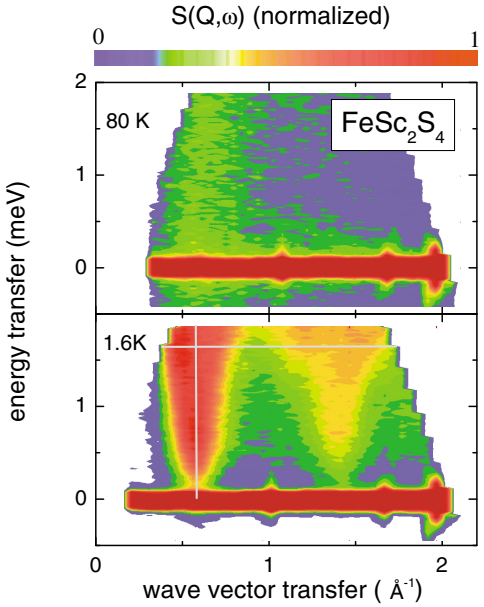

FIG. 4 (color). Contour plot of $S(Q, \omega)$ of $FeSc_2S_4$ in the low-Q and low-energy region at $T = 80$ K (upper panel) and $T = 1.6$ K (lower panel). The full lines indicate a constant-Q scan at 0.6 $Å^{-1}$ and a constant-energy scan at $\hbar\omega = 1.6$ meV, respectively, shown in Fig. 5.

without any splitting that would indicate a structural transition. Moreover, we note that even at 1.6 K there are no indications of magnetic Bragg reflections. At 80 K, $S(Q, \omega)$ of $FeSc_2S_4$ reveals the typical features of antiferromagnetic spin fluctuations of purely relaxational type, peaked at zero energy transfer. In contrast, $S(Q, \omega)$ at 1.6 K reminds us of a liquid close to condensation. The remarkable feature is the low-energy magnetic response that appears especially strong at $Q = 0.6$ $Å^{-1}$. This Q value just corresponds to the (100) reflection which is forbidden in space group $Fd\bar{3}m$ describing the symmetry of the spinel structure. However, the (100) reflection will show up for a simple AFM coupling that removes the face centering. Therefore, magnetic intensity around $Q = 0.6$ $Å^{-1}$ indicates the presence of AFM spin fluctuations. As documented in the upper panel of Fig. 4, these are present already well above the expected mean-field ordering temperature of $\Theta_{CW} \simeq 45$ K, estimated from the Curie-Weiss law of the susceptibility [11], but on cooling, their character changes dramatically despite the fact that $FeSc_2S_4$ remains paramagnetic. The dynamic response at this characteristic Q value shows a marked temperature dependence that is depicted in the constant-Q strip of Fig. 5 (lower frame). In the high-T range the energy dependence appears as a rather continuous level evidencing a quasielastic response (see also the upper panel of Fig. 4). There is a notable increase of the low-energy response in the range 1 to 2 meV. Nevertheless, the main response remains separated from the elastic line by a gaplike dip of about 0.2 meV even at the lowest temperature observed.

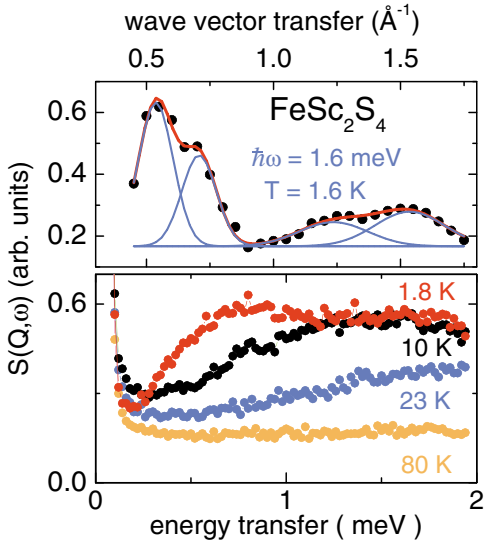

FIG. 5 (color online). Constant-energy scan at $\hbar\omega = 1.6$ meV and $T = 1.6$ K (upper panel) and constant-Q scans at 0.6 Å^{-1} for various temperatures (lower panel), respectively.

The dynamic response of frustrated 3D magnetic systems investigated so far exhibits short-range correlations of quasielastic origin, with no indications of either a spin gap or well defined magnetic excitations. The geometrically frustrated pyrochlore $Tb_2Ti_2O_7$, with a Curie-Weiss temperature of -19 K, remains paramagnetic down to 0.07 K. There the lowest lying crystal-field excitation of Tb^{3+} develops a very moderate dispersion near the first maximum of the magnetic structure factor only [23]. In $FeSc_2S_4$ at low temperatures, strongly dispersive spin excitations develop as illustrated in the upper part of Fig. 5, where a constant-energy strip at $\hbar\omega = 1.6$ meV reveals a double peak structure. However, these excitations remain broad in Q (the width corresponds to some three unit cells correlation length) and energy, more reminiscent of the continuum response of some low-dimensional quantum antiferromagnets indicating a liquidlike structure factor. The full bandwidth of the magnetic response is consistent with the Curie-Weiss temperature; therefore, the nearest neighbor exchange coupling must be of the order of 0.5 to 1 meV. We suggest that the gap of the order of 0.2 meV is a characteristic ingredient of this particular SL in the sense that in absence of symmetry breaking there is no mode starting from zero energy. Therefore, a slight anisotropy which might contribute to the gap of an ordered state can be excluded due to the orbital liquid state. Thus our results demonstrate that $FeSc_2S_4$ shows a very specific dynamic response associated with its SOL character. Its tendency to spin order is suppressed, and in spite of the notable softening, the magnetic response remains dynamic in the examined temperature range.

To conclude, our results demonstrate that in $FeSc_2S_4$ the orbital doublet remains degenerate but is strongly coupled to vibronic modes with a vibronic splitting $\Gamma = 2$ meV. This excitation can be explained in terms of a dynamic Jahn-Teller effect including spin-orbit coupling [20]. The spin system reveals a crossover from a system with strong AFM spin fluctuations with a purely relaxational excitation spectrum at $T > \theta_{CW}$ to a cooperative paramagnet with isotropic magnonlike excitations at low temperatures ($T \leq \theta_{CW}$). The orbital disorder seems to play an essential role in establishing the spin-liquid state.

This work was supported by the BMBF under Contract No. 13N6917 (EKM) and by the DFG via Sonderforschungsbereich 484, Augsburg. We thank J. Hemberger for providing Fig. 1.

[1] H. A. Jahn and E. Teller, Proc. R. Soc. A **161**, 220 (1937).
[2] K. I. Kugel and D. I. Khomskii, Sov. Phys. Usp. **25**, 231 (1982).
[3] K. Binder and A. P. Young, Rev. Mod. Phys. **58**, 801 (1986).
[4] A. P. Ramirez, in *Handbook of Magnetic Materials*, edited by K. H. J. Buschow (Elsevier, New York, 2001), Vol. 13, pp. 423–520.
[5] R. Ballou, E. Lelièvre-Berna, and B. Fåk, Phys. Rev. Lett. **76**, 2125 (1996).
[6] A. Krimmel *et al.*, Phys. Rev. Lett. **82**, 2919 (1999).
[7] S.-H. Lee *et al.*, Nature (London) **418**, 856 (2002).
[8] S. T. Bramwell and M. J. P. Gingras, Science **294**, 1495 (2001).
[9] A. P. Ramirez *et al.*, Nature (London) **399**, 333 (1999).
[10] R. Fichtl *et al.*, Phys. Rev. Lett. **94**, 027601 (2005).
[11] V. Fritsch *et al.*, Phys. Rev. Lett. **92**, 116401 (2004).
[12] H. Nakamura *et al.*, J. Phys. Condens. Matter **9**, 4701 (1997).
[13] J. R. Stewart *et al.*, Phys. Rev. Lett. **89**, 186403 (2002).
[14] S.-H. Lee *et al.*, Phys. Rev. Lett. **86**, 5554 (2001).
[15] A. P. Murani *et al.*, J. Phys. Condens. Matter **16**, S607 (2004).
[16] W. L. Roth, J. de Physique et de le Radium **25**, 507 (1964).
[17] M. Mücksch *et al.* (to be published).
[18] F. S. Ham, in *Electron Paramagnetic Resonance*, edited by S. Gschwind (Plenum, New York, 1972).
[19] G. A. Slack *et al.*, Phys. Rev. **187**, 511 (1969).
[20] L. F. Feiner, J. Phys. C **15**, 1515 (1982).
[21] C. Testelin *et al.*, Phys. Rev. B **46**, 2183 (1992).
[22] L. Brossard, H. Oudet, and P. Gibart, J. Phys. (Paris), Colloq. **6**, C493 (1976).
[23] J. S. Gardner *et al.*, Phys. Rev. Lett. **82**, 1012 (1999).